JOURNAL OF MATERIALS SCIENCE 32 (1997) 2821–2826

Overlapping laser tracks to produce a continuous nitrided layer in Ti–6Al–4V alloy

C. HU, T. N. BAKER
Metallurgy and Engineering Materials Group, Department of Mechanical Engineering, University of Strathclyde, Glasgow G1 1XN, UK

Continuously overlapping a number of tracks resulted in a significant influence in laser nitriding of a Ti–6Al–4V alloy. Not only was the microstructure in the overlapped areas found to be different from that in the non-overlapped areas, but also the microstructures developed by successive tracks could influence each other, especially for the first few laser tracks. Moreover, the melt-pool depth and profile changed with the sequence number of the overlapped tracks. This resulted in a non-uniform surface layer and therefore non-uniform surface properties. The correlations between the processing parameters and melt-pool depth and hardness were determined, which leads to a method or principle for the design and control of the processing whenever track overlapping is required. A second important consideration is the effect of specimen thickness on the resultant microstructure. A CO_2 continuous spinning laser beam was used in this work.

1. Introduction

Laser nitriding of titanium alloys has been investigated extensively in recent years with the aim of improving the material surface properties, especially the hardness, the wear resistance and the erosion resistance [1–10]. A wide research area has been explored in the processing, which includes the improvement of the surface properties, the analysis of the residual stress and cracking induced in the material, the melt-pool depth and profile developed by the beam, and the microstructural characterization. The hardness was reported to reach 1800 H_V, when a commercial purity titanium alloy was treated by a CO_2 laser with a Gaussian energy distribution under a nitrogen environment [8]. The wear resistance significantly increased [4], the residual stress was reduced and cracking eliminated when a dilute nitrogen environment was used for the processing [10]. All of these aspects have shown promising results and a great potential for the application of this process into industry.

However, most of the results obtained in the previous work [10] were from single-track experiments. An important and necessary step to the practical application of this process is to overlap a number of the laser tracks to produce a continuous modified layer in a specific area on the surface. In other words, the surface layer produced by a number of overlapped tracks may not be the same as that which would have been produced by a single track and confirmed to be satisfactory for a specific need. To determine the influence of the overlapping of the tracks in the laser nitriding process with the aim of producing a continuous and uniform surface layer, the present work, using a CO_2 continuous 5 kW laser in the spinning beam mode, investigated the laser nitriding of Ti–6Al–4V with eight overlapping tracks. The microstructure resulting from track overlapping was characterized, the melt-pool depth and profile changes were examined, and the influences of and the interactions between the processing parameters were discussed. Some new processing parameters were found to be important when track overlapping was employed, and therefore are emphasized in this work and suggested to be used together with the laser processing conditions for the control of the overlapping process. Based on the influences of the laser track overlapping on the microstructural variations through the melt zone, and the correlation between the processing parameters and the experimental results, consideration was given to the modified parameters essential to the design of the laser track overlapping. These considerations are applicable to other laser surface treatments whenever the track overlapping technique is employed.

2. Experimental procedure

A CO_2 continuous 5 kW laser, at AEA Technology, Culham, UK, was used. The beam had an annular shape and the energy was uniformly distributed in an annular area when the beam was in a stationary state. In the spinning beam mode, the radius of the spinning locus, (r_s), was set at 2 mm and the velocity of the spinning at 1500 r.p.m. for all the experiments in the present work. The laser power, q, was set at 3.7 kW, the specimen velocity, v, at 3 mm s^{-1}.

A Ti–6Al–4V alloy (IMI 318) was used as the base alloy to be nitrided. The specimens were ground with 500 grit paper and cleaned with methanol before the nitriding. During the treatments, the specimens were

0022–2461

moved under the laser on a work table with the surfaces to be treated at a defocused distance (DFD) of 15 mm above the focal point. Three levels of the specimen thickness (4, 10 and 18 mm) were used, and the dimensions of the surface were 100 mm × 100 mm.

The nitriding environment used was 40 vol % nitrogen with the balance argon gas, with a gas flow of 10 min^{-1}; 35% was chosen as the overlapping fraction. To ensure the accuracy of the 35% overlapping, a single track was made and the width measured, and then the distance between every two tracks decided for eight continuously overlapped tracks. A constant time interval of 35 ± 5 s was taken between every two tracks (from the end of a track to the start of the following one). The microstructure, the melt-pool depth and the profile of the transverse section were examined on both an optical and a scanning electron microscope (SEM). The phases formed in the surface layer were determined by X-ray diffractometry. The hardness of the surface was measured on the transverse section of the specimens using a Mitutoyo MVK-G1 microhardness tester with a load of 100 g, and given as a function of the distance from the surface.

3. Results and discussion

3.1. Melt-pool depth

Under the experimental conditions described above, a correlation between the melt depth and the sequence number of the overlapped tracks was found and is shown in Fig. 1. The melt depth increased with the number of the track until a constant value of the depth was reached. Under identical processing conditions, the deepest melt depth was produced in the 4 mm specimen, the second deepest in the 10 mm specimen and the shallowest in the 18 mm specimen. The melt depth produced by the first track is considered to be the same as that produced by a single track. A single track would have produced under identical processing conditions a constant melt depth if the thickness of the specimen was above a critical value, which can be treated as a semi-infinite plate. Any thickness less than the critical value will give a deeper melt depth than that which would be obtained on a semi-infinite plate. It is clear from Fig. 1 that the difference in the melt depth between the three specimens also increased with the sequence number of the tracks. In other words, the melt depth produced in a thinner specimen increased more significantly than in a thicker specimen. This is attributed to the preheating effect of the previous laser tracks. All the specimens had the same initial temperature (room temperature) prior to the melting of the first laser track. Under identical processing conditions, all the three specimens absorbed the same energy input from the first track. The same amount of energy developed by the laser for the different thicknesses of specimens resulted in different initial temperatures in the material prior to the melting of the second track, and the thinner the specimen, the higher the temperature, unless the time interval between the melting of the two tracks was sufficiently long to allow the temperatures to fall to room temperature. On the other hand, the higher the temperature of the specimen, the greater the energy transferred from the specimen to the surroundings during a constant time interval. Because the processing conditions were identical and the energy absorption was independent of temperature [11], the laser energy input to each track was constant. However, the energy output increased as the number of tracks increased, but when the heat input balanced the heat removed, which occurred after a critical number of tracks had been melted, the melt depth reached a constant value. This number was dependent on the processing conditions, the thickness and/or the size of the specimen and the time interval between the tracks.

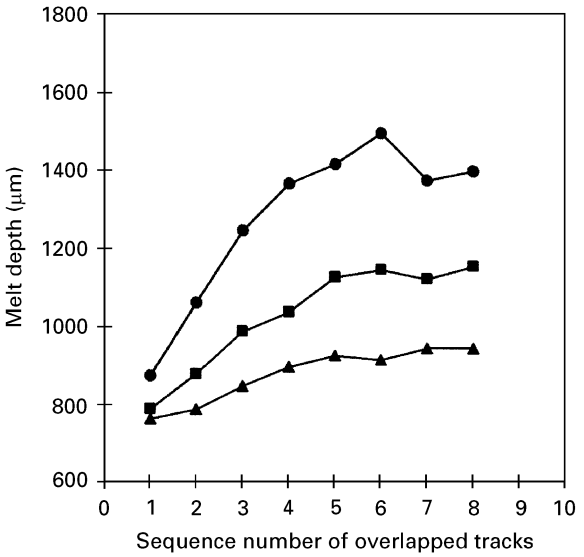

Figure 1 The correlation between the melt depth and the sequence number of the tracks during an overlapping process; using a spinning beam at $q = 3.7$ kW, $v = 3$ mm s^{-1}, DFD = 15 mm, $r_s = 2$ mm and a time interval of 35 ± 5 s under 40% N: (●) 4 mm thick, (■) 10 mm thick, and (▲) 18 mm thick specimens.

It was observed that not only the melt depth increased but also the melt-pool profile changed significantly with succeeding tracks from that produced by the first track. This resulted in an unexpected non-uniformity of the surface layer, especially when the overlapping fraction had been designed according to the melt profile produced by a single track. Fig. 2 shows the overlapped area of tracks one and two in the 4 mm specimen, and Fig. 3 that of tracks four and five for identical processing conditions. Obviously, the melt depth as shown in Fig. 3 has increased significantly, but the uniformity of the melt depth decreased compared with that in Fig. 2. For simplicity in the following discussion, the uniformity of the melt depth is defined as the ratio of the shallowest depth (at the overlapped area) to the deepest (in the centre of the melt pool) produced by the first of the two overlapped tracks. Therefore, the uniformity of the melt depth in Fig. 2 is 0.75, and that in Fig. 3 is 0.6.

Generally, using a large overlapping fraction gives a more uniform melt depth, but requires more tracks to cover the same area compared to the situation of using a small overlapping fraction. An unnecessarily large overlapping fraction will cost more laser time and energy. Therefore, an optimum overlapping

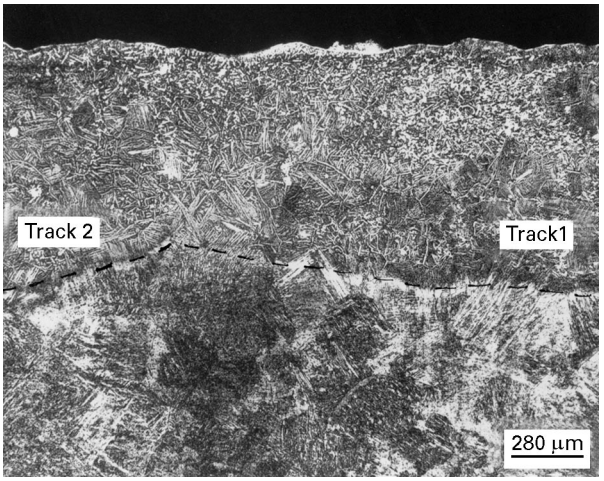

Figure 2 The overlapped area of the first and second tracks on the 4 mm specimen, showing the uniformity of the melt depth in the area of 0.75.

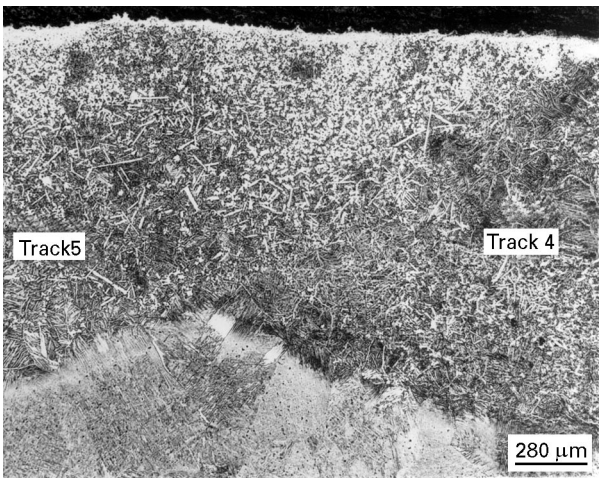

Figure 3 The overlapped area of the fourth and fifth tracks on the 4 mm specimen, showing the uniformity of the melt depth in the area of 0.6.

fraction should be designed according to the melt profile. In our previous work, the temperature field developed by a single track of a spinning beam on a semi-infinite plate was calculated using a line-source method associated with superposition [12, 13]. Three possible melt-pool profiles on the transverse section produced by a spinning beam are given schematically in Fig. 4. If the laser input is low, the melt profile developed can be shown by curve 1 in Fig. 4. The melt depth is non-uniform and is shallowest at the beam centre. When a specific level of laser input is used, a constant melt depth within a certain distance in the middle of the melt pool can be produced. This is shown by curve 2 in Fig. 4. Any other laser input levels higher than this will result in a melt profile similar to curve 3 in Fig. 4 in which the melt depth is non-uniform and the deepest melt is located at the centre of the melt pool. It can be seen from Fig. 4 that the melt profile of curve 2 will give the most uniform melt depth when laser tracks are overlapped and a minimum overlapping fraction is used. Based on our previous work [13], the minimum overlapping fraction was calculated to be 0.35 when a spinning beam is

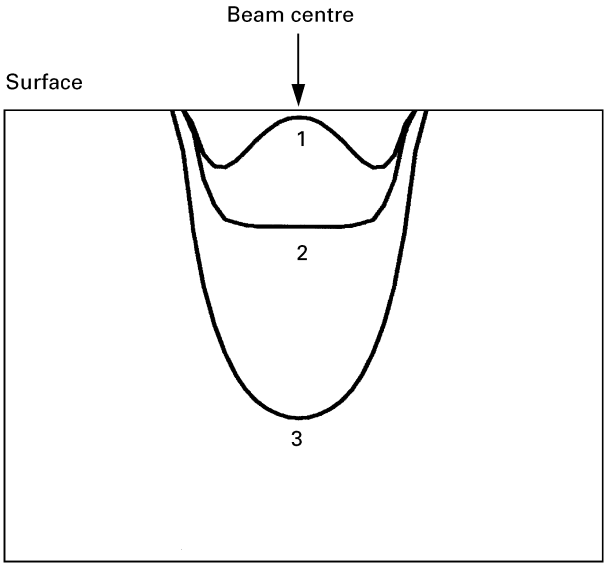

Figure 4 Three possible melt-pool profiles developed by a spinning beam.

used. In practice, it is very difficult to control the process to obtain the melt profile like that of curve 2 in Fig. 4, and most melt pools produced by a spinning beam have a profile between curves 2 and 3. In these cases, the higher the energy input, the larger the overlapping fraction needed. Because the melt profile produced by each of these continuously overlapped tracks is different, the design of the overlapping process should be based on the constant melt profile after a number of tracks. This requires a determination of the processing conditions necessary to produce a constant melt pool which has a similar profile to that shown by curve 2 in Fig. 4 and then to determine an optimum overlapping fraction according to the melt profile. Therefore, further work modelling the overlapping process is required to predict and optimize the constant melt profile. However, the overlapping fraction will always be $\geqslant 0.35$ when a spinning beam is used. This figure is less than the minimum used by Robinson *et al.* [9] and significantly lower than the 75% overlapping suggested by Morton *et al.* [4] as an optimum for producing an alloyed layer with a homogeneous microstructure.

3.2. Hardness

Because the melt depths and profiles produced by the tracks were not constant during continuous overlapping, neither were the hardness profiles in this surface layer. The hardness was measured as a function of the distance from the surface in the centre of the melt zone for all the tracks. For a clear presentation and a simple discussion, only the hardness profiles in the three tracks (numbers 1, 4 and 8 in order of overlapping) from the 18 mm specimen are shown in Fig. 5. First, the hardness in the melt increased significantly compared with the matrix of the base alloy and therefore a deeper melt coincided with a thicker surface layer of a high hardness. Second, a deeper melt resulted in a higher hardness, particularly at the top of the surface. It is considered that a deeper melt coincided with

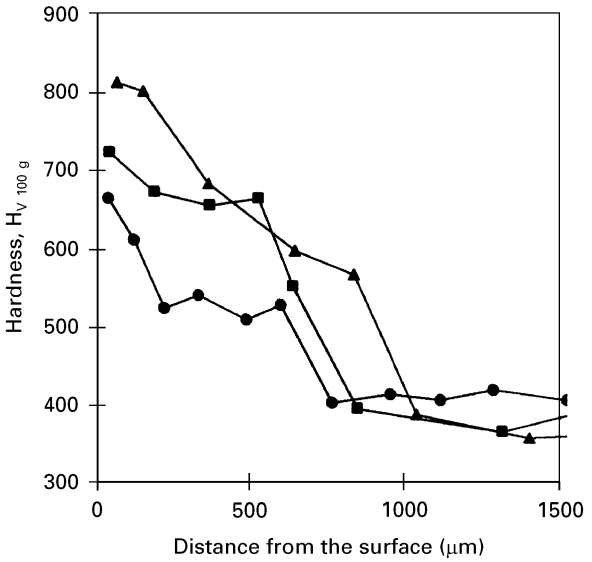

Figure 5 Hardness profiles as a function of the distance from the surface obtained from tracks (●) 1, (■) 4 and (▲) 8 on the 18 mm specimen.

a higher temperature on the surface, a longer liquid life time and therefore a larger amount of nitrogen which reacted with and diffused into the liquid. It can be seen from Fig. 5 that a maximum hardness was achieved at the top of the surface, the hardness dropped dramatically at a short distance from the surface, and then reduced gradually until the area near to the bottom of the melt, where an almost constant hardness was found. It is understood that the increase in hardness resulted mainly from the formation of titanium nitrides and maybe also, to a limited extent, from the solid solution of nitrogen in the Ti–6Al–4V alloy. However, the hardness is related to the microstructure. Therefore, the microstructure of the surface was characterized by microscopy and X-ray diffractometry.

3.3. Microstructure

An X-ray spectrum from the surface, as shown in Fig. 6, confirmed that the titanium nitride which formed in the top layer was TiN. Two optical micrographs in Figs 2 and 3 show that a high concentration of titanium nitride (white phase) formed in the top layer and the concentration decreased with distance from the surface, but the rate of decrease was obviously not uniform in the direction of melt depth. The high concentration of titanium nitride on the surface occurred because the nitrogen was in direct contact with the liquid at the surface, and the non-uniform reduction rate of the titanium nitride concentration is attributed to the convection flow generated in the liquid during the processing. Furthermore, the concentration of titanium nitride particles increased with an increase in the sequence number of tracks. This can be related to the dependence of hardness on the track position.

The scanning electron micrograph in Fig. 7 shows that the titanium nitride particles in the top area had an angular complex shape and were interconnected.

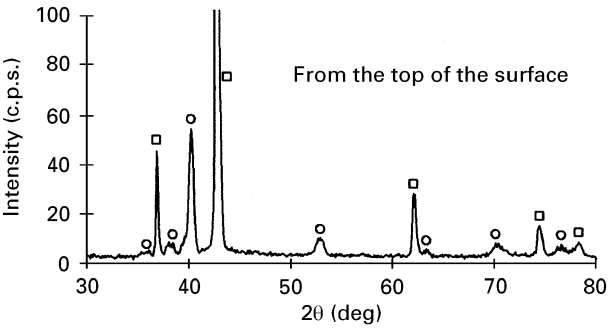

Figure 6 An X-ray diffractometry spectrum from the surface of the above specimen showing the TiN formed in the top area; (□) peaks of TiN, (○) peaks of α-Ti.

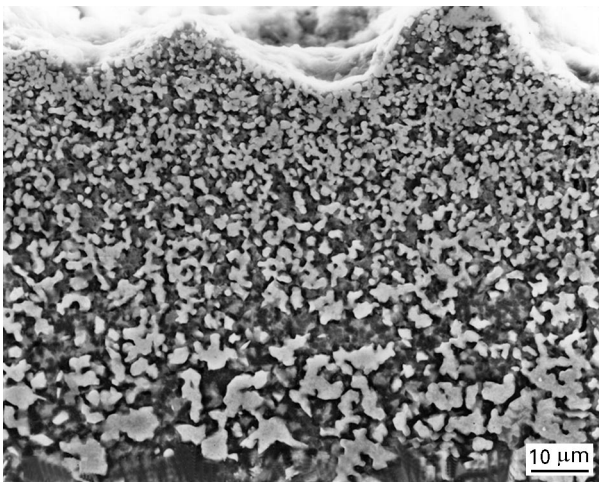

Figure 7 Scanning electron micrograph showing complex titanium nitride particles formed and connected with each other in the top region of the surface; taken from the top region of track 4 of the 4 mm thick specimen under the conditions of $q = 3.7$ kW and 40% N.

These particles had the finest size at the top and the size increased with the distance from the surface. This morphology of TiN shown in Fig. 7 was observed in all the three thicknesses of the specimens, and is significantly different from that of our previous work, an example of which is seen in Fig. 8. For the same alloy (Ti–6Al–4V) and the same spinning beam conditions used in the processing, a low laser power (2.8 kW) and a high nitrogen concentration (100% N) produced titanium nitride dendrites whose primary arms were perpendicular to the surface. This different morphology of nitrides during a solidification is considered to be due to different mechanisms of formation. When a low laser energy input and a high nitrogen environment were used, a high cooling rate in the solidification stage of the material and a high concentration of nitrogen on the liquid surface would be expected. Although the temperature at the surface was the highest in the melt, the liquid at the surface could have the highest undercooling, because of the high concentration of nitrogen in the surface liquid whenever the surface temperature was below the melting point of TiN (2930 °C) [14]. Therefore, solidification could occur from the surface, with the formation of titanium nitrides, when most of the melt pool was still in the

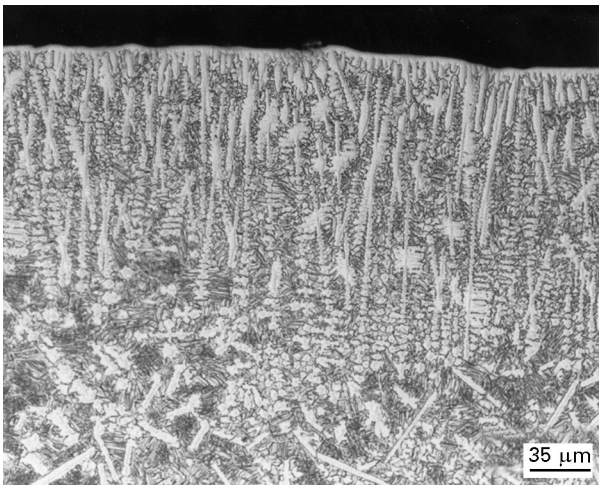

Figure 8 Titanium nitride dendrites perpendicular to the surface formed: a single track under the conditions of $q = 2.8$ kW and 100% N.

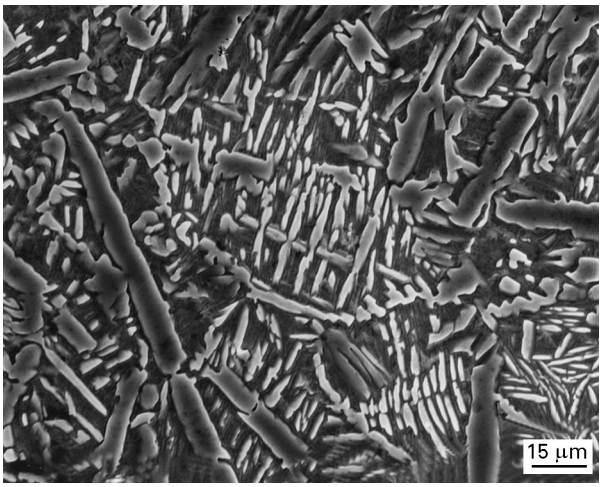

Figure 9 Scanning electron micrograph showing a mixture of the complex TiN particles, the needles of $TiN_{0.3}$ and the martensite of the matrix of base alloy; taken from the centre region of the same specimen as that for Fig. 7.

liquid state. Moreover, a high and negative temperature gradient in the liquid ahead of that in which TiN particles had already formed, encouraged the particles to grow in the direction of the maximum undercooling, i.e. perpendicular to the surface, and resulted finally in the formation of the titanium nitride columnar dendrites. This situation did not exist when the laser energy input was high (3.7 kW) and the nitrogen concentration in the environment was low (40% N). It is thought that when the surface was cooled to a temperature just below 2930 °C, the nitrogen concentration in the liquid surface might be too low to form TiN, and when the temperature was sufficiently low to form TiN, the quantity of the remaining liquid and the temperature gradient in the liquid did not allow a significant quantity of columnar dendrites to form. The formation of the columnar dendrites should be taken as a sign of the surface solidification occurring while most of the melt region was still liquid.

Below the top layer of TiN there was a layer containing a mixture of the TiN particles and some needle particles, together with a matrix of a martensitic phase of the base alloy, as shown in Fig. 9. The needle phase has been reported to have a hexagonal crystal structure, and was considered to be $TiN_{0.3}$ [10, 15]. The fraction of TiN, in general, decreased with distance from the surface. However, high fractions may occur locally due to the effect of convection.

It should be noted that the track overlapped areas had a deeper top layer and a higher density of TiN in this layer, as well as a shallower melt depth, compared with the non-overlapped areas. The profile of the top layer which contains TiN depends mainly on the second laser track. This can be seen in Fig. 3. Obviously, the effects of these microstructural characteristics on the surface properties, such as wear and erosion resistance, may be considerable and will be studied in the near future. Whenever necessary, data from these tests will be incorporated into the design of the overlapping fraction.

3.4. Cracking

Cracking is a critical problem in deciding the processing parameters, and is associated with the titanium nitride phase [4, 16] and the residual stress [4] induced by the rapid cooling rate which occurs during laser processing. Therefore, any factor which affects either the quantity of the titanium nitride or the residual stress will have an influence on the tendency to cracking. A diluted nitrogen environment reduces the quantity of TiN and $TiN_{0.3}$ [15], and a high laser power and a low beam speed are expected to reduce the cooling rate in the solid state by increasing the energy input and therefore reducing the residual stress. For this reason the following parameters, 40% N in the gas, 3.7 kW laser power and 3 mm s^{-1} beam speed, were used in the present work. No cracking was observed in any of the tracks in either the 4 or 10 mm thick specimens. In the 18 mm specimen, cracking occurred in tracks 1–7, but not in the eighth track. This indicates that the thickness of the specimen has a very important effect on cracking, and the thicker the specimen, the higher is the tendency to crack when the laser conditions are constant. Cracking can be avoided by preheating the specimen, which will also reduce the cooling rate [4]. For example, under the experimental conditions in the present work, preheating the 18 mm specimen to the same temperature as that reached prior to the eighth track, should eliminate cracking on the surface. On the other hand, Robinson *et al.* [17] deliberately designed some experiments in which each overlapped track was allowed to cool below 50 °C before carrying out the following pass. This was to avoid the effect of preheating on residual stress. Cracking was observed even with dilute nitrogen atmospheres (20%) in 10 mm thick specimens. Tensile residual stresses reached a maximum with the fourth and fifth overlapped tracks, before decreasing to a compressive state with track eight.

3.5. Considerations in designing an overlapping process

From the above discussion, it is considered that single-track experiments will provide information on the minimum melt-depth and melt-pool size, the smallest quantity of titanium nitride particles and the lowest hardness of a crack-free surface layer produced under a given set of processing parameters. The correlations shown above can be used as a guide to choose the parameters for overlapping of tracks, such as the time interval between laying down of successive tracks, the laser conditions and the nitrogen concentration to optimize the melt profile and hardness gradient. Once this has been achieved for a specific application, an optimum overlapping fraction should then be determined to achieve a uniform surface layer. If the specimen is virtually free of cracks, the region of the earliest formed tracks which may have produced a less satisfactory layer, can be reprocessed. When cracking is observed in the area of the early tracks, preheating the specimen to the same temperature as that prior to the critical track which produced a crack-free and satisfactory surface layer, will eliminate the cracking in other specimens. Because the correct preheating temperature is difficult to ascertain, a simple and accurate method is to preheat the specimen using the same laser under identical conditions using an argon or helium gas, for the same number of tracks (here the difference between the energy absorption under the nitrogen and argon or helium is considered to be negligible).

4. Conclusions

1. Sequentially overlapping laser track experiments using a continuous 5 kW CO_2 laser were conducted on a Ti–6Al–4V alloy in this work and found to produce significantly different melt depths, melt profiles, microstructure and hardness, from those developed by a single-track experiment using similar conditions.

2. The correlation between the melt depth and the sequence number of the overlapped tracks is described in this work, which is dependent on the time intervals between producing the tracks, the thickness of the specimen and the laser-processing conditions.

3. An optimum overlapping fraction giving a better uniformity of the surface layer, should be determined according to the constant melt profile developed after a number of overlapped tracks instead of using a single-track melt profile.

4. A high laser energy input and a low nitrogen concentration resulted in a complex angular shape of TiN particles, and a low-energy input and high nitrogen concentration columnar dendrites. This indicates that there are at least two possible mechanisms of formation of the TiN particles during the processing.

5. The thicker the specimen in the range 4–18 mm, the greater is the tendency to cracking, but cracking may be avoided by preheating the specimen.

Acknowledgements

The authors gratefully acknowledge EPSRC/DTI, for the financial support through the award of a Link Advanced Surface Engineering grant. Thanks are also extended to Dr J. Fieret, Mr G. Baker and Mr R. Heath, AEA Technology, Culham, for assistance in the operation of the laser, and to Mr H. Xin and Mr H. How, University of Strathclyde, for assistance with X-ray diffractometry and SEM.

References

1. C. W. DRAPER and J. M. POATE, *Int. Met. Rev.* **30** (1985) 28.
2. A. WALKER, J. FOLKES, W. M. STEEN and D. R. F. WEST, *Surf. Eng.* **1** (1985) 23.
3. S. MRIDHA and T. N. BAKER, *Mater. Sci. Eng.* **A142** (1991) 115.
4. P. H. MORTON, T. BELL, A. WEISHEIT, J. KROLL, B. L. MORDIKE and K. SAGOO, in "Surface Modification Technologies V", edited by T. S. Sudarshan and J. F. Braza (Institute of Materials, London, 1992) p. 593.
5. V. M. WEERASINGHE, D. R. F. WEST and M. CZAJLIK, *Mater. Sci. Forum* **102–104** (1992) 401.
6. S. MRIDHA and T. N. BAKER, *Mater. Sci. Eng.* **A188** (1994) 229.
7. J. M. ROBINSON and R. C. REED, *Wear* **186–187** (1995) 360.
8. A. B. KLOOSTERMAN and J. Th. M. DE HOSSON, *Scripta Metall. Mater.* **33** (1995) 567.
9. J. M. ROBINSON, S. ANDERSON, R. D. KNUTSEN and R. C. REED, *Mater. Sci. Technol.* **11** (1995) 611.
10. C. HU, S. MRIDHA, H. S. UBHI, A. W. BOWEN and T. N. BAKER, in "Titanium'95: Science and the Technology," edited by P. A. Blenkinsop, W. J. Evans and H. M. Flower (Institute of Materials, London, 1996) p. 2835.
11. T. J. WIEITING and J. T. DCHRIEMPF, *J. Appl. Phys.* **47** (1976) 4009.
12. C. HU and T. N. BAKER, in "Proceedings of 5th International Conference on Improvement of Materials", MATEC, edited by J. Liu (Marne La Vallee, Paris, 1996) p. 167.
13. C. HU and T. N. BAKER, *Metall. Mater. Trans.* **27A** (1996) 4039.
14. R. C. WEAST and M. J. ASTLE (eds), "Handbook of Chemistry and Physics" 61st Edn (CRC Press, Boca Raton, Fl, 1980).
15. H. XIN and T. N. BAKER, in "Titanium'95: Science and the Technology," edited by P. A. Blenkinsop, W. J. Evans and H. M. Flower (Institute of Materials, London, 1996) p. 2031.
16. S. MRIDHA and T. N. BAKER, *Proc. Adv. Mater.* **4** (1994) 85.
17. J. M. ROBINSON, B. A. VAN BRUSSEL, J. TH. M. DE. HOSSON and R. C. REED, *Mater. Sci. Eng.* **A208** (1996) 143.

Received 23 August 1996
and accepted 7 January 1997